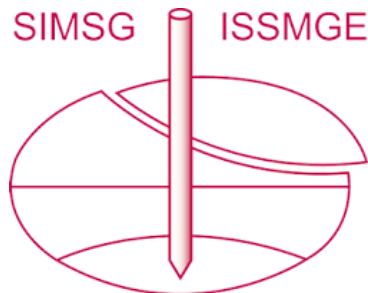


INTERNATIONAL SOCIETY FOR SOIL MECHANICS AND GEOTECHNICAL ENGINEERING



This paper was downloaded from the Online Library of the International Society for Soil Mechanics and Geotechnical Engineering (ISSMGE). The library is available here:

[*https://www.issmge.org/publications/online-library*](https://www.issmge.org/publications/online-library)

This is an open-access database that archives thousands of papers published under the Auspices of the ISSMGE and maintained by the Innovation and Development Committee of ISSMGE.

Effects of measurement profile configuration on estimation of stiffness profiles of loose post glacial sites using MASW

E. Á. Ólafsdóttir

*Faculty of Civil and Environmental Engineering, University of Iceland, Reykjavík, Iceland,
eao4@hi.is*

S. Erlingsson, B. Bessason

Faculty of Civil and Environmental Engineering, University of Iceland, Reykjavík, Iceland

ABSTRACT

Post glacial loose surface sediments are common in Iceland. Knowledge of the geotechnical properties of these sites is essential in various civil engineering projects. The shear wave velocity is a key parameter in this sense. Multichannel Analysis of Surface Waves (MASW) is a new and advanced technique to estimate shear wave velocity profiles of soil sites. The MASW method has been applied at two loose sites close to Landeyjahöfn harbour in South Iceland. The MASW field measurements were performed using twenty-four 4.5 Hz geophones as receivers spaced between 0.5 and 2 m apart. A 6.3 kg sledgehammer and jumping were used as impact sources. For each receiver setup, up to seven different source offsets were used, ranging from 5 to 50 m. Fourier analysis and phase velocity scanning was applied to evaluate dispersion curves based on data acquired with diverse receiver setups in order to assess the effects of the receiver spacing and the source offset on the quality of the surface wave records. The results indicate that the configuration of the MASW measurement profile has a substantial effect on the acquired time series and that it is beneficial to combine dispersion curves obtained from several different records which have been gathered at the same site prior to the inversion analysis.

Keywords: Multichannel Analysis of Surface Waves (MASW), field measurements, measurement profile configuration, dispersion analysis, shear wave velocity.

1 INTRODUCTION

Post glacial loose surface sediments of different nature are common in Iceland. Knowledge of the geotechnical properties of these sites is essential in various civil engineering projects. The shear wave velocity is a key parameter in this sense. The stiffness of individual soil layers is directly proportional to the square of their characteristic shear wave velocity. Furthermore, the shear wave velocity is vital in both liquefaction potential and soil amplification assessments (Kramer, 1996) and when defining site specific earthquake design loading according to Eurocode 8 (CEN, 2004).

For two decades, the seismic exploration method Spectral Analysis of Surface Waves

(SASW) has been applied in Iceland to estimate the shear wave velocity and stiffness profiles of soil sites (Bessason, Baldvinsson and Þórarinsson, 1998; Bessason and Erlingsson, 2011). The Multichannel Analysis of Surface Waves (MASW) is a relatively new and more advanced technique. Implementation of the MASW method in Iceland began in 2013 (Ólafsdóttir, Bessason and Erlingsson, 2015). The first MASW measurements were carried out in South Iceland and a new set of software tools for analysis of MASW field data is under development at the Faculty of Civil and Environmental Engineering, University of Iceland (Ólafsdóttir, 2016).

The objective of the study presented in this paper is to develop and customise the new MASW method. This includes evaluation of the effects of the measurement profile configuration on the quality of the acquired surface wave records, as well as further development of the set of software tools used to carry out the analysis of the MASW field data.

2 MASW

In MASW, Rayleigh waves are generated and used to infer the shear wave velocity profile of the test site as a function of depth (Park, Miller and Xia, 1999). Compared to other available methods, surface wave analysis methods are low-cost, as well as being non-invasive and environmentally friendly since they neither require heavy machinery nor leave lasting marks on the surface of the test site.

The main advantages of the MASW method over the SASW method include a more efficient data acquisition routine in the field, faster and less labour consuming data processing procedures and improved identification and elimination of noise from recorded data (Park et al., 1999; Xia et al., 2002). Furthermore, observation of stiffness properties as a function of both depth and surface location becomes possible and economically feasible by using MASW (Xia, Miller, Park and Ivanov, 2000). Finally, it is possible to map significantly deeper shear wave velocity profiles when using the same impulsive source, i.e. a reasonably heavy sledgehammer. The observed difference between results obtained by MASW and direct borehole measurements is approximately 15% or less and random (Xia et al., 2002).

The maximum depth of investigation in a MASW survey varies with site, the natural frequency of the geophones that are used in the field measurements and the type of seismic source that is used. The investigation depth is determined by the longest Rayleigh wave wavelength that is obtained during data acquisition. A commonly adopted empirical criterion (Park and Carnevale, 2010) is that:

$$z_{max} \approx 0.5\lambda_{max} \quad (1)$$

where z_{max} (m) is the investigation depth and λ_{max} (m) is the longest wavelength.

MASW surveys can be broken down into three steps; field measurements, dispersion analysis and inversion analysis (Park et al., 1999). A general overview of the three-step procedure is provided in Fig. 1.

2.1 Field measurements

For field measurements, low frequency geophones are lined up on the surface of the test site as shown in Fig. 1a. For active MASW surveys (Park, Miller, Xia and Ivanov, 2007), which are the focus of this study, a wave is generated by an impulsive source that is applied at one end of the measurement profile. The geophones record the resulting wave propagation as a function of time (Fig. 1b). The distance from the impact load point to the first receiver in the geophone line up is referred to as the source offset and denoted by x_1 (see Fig. 1a). The receiver spacing is dx and the number of receivers is n . Hence, the length of the receiver spread is $L = (n - 1)dx$ and the total length of the measurement profile is $L_T = x_1 + (n - 1)dx$.

2.2 Dispersion analysis

In the dispersion analysis, Rayleigh wave dispersion curves are obtained using the recorded time series. Here, the so-called phase shift method (Park, Miller and Xia, 1998) is employed to obtain a dispersion image (a phase velocity spectrum). The dispersion image visualizes the dispersion properties of all types of waves contained in the recorded time series in the frequency – phase velocity domain. Different modes of Rayleigh waves are recognized by their frequency content and characterizing phase velocity at each frequency. Noise sources, e.g. body waves and reflected/scattered waves, are likewise recognized by their frequency content.

The phase shift method can be divided into three steps; Fourier transformation and amplitude normalization, dispersion imaging and extraction of dispersion curves (Park et al., 1998). The three main data processing steps are illustrated in Fig. 2 and briefly described below.

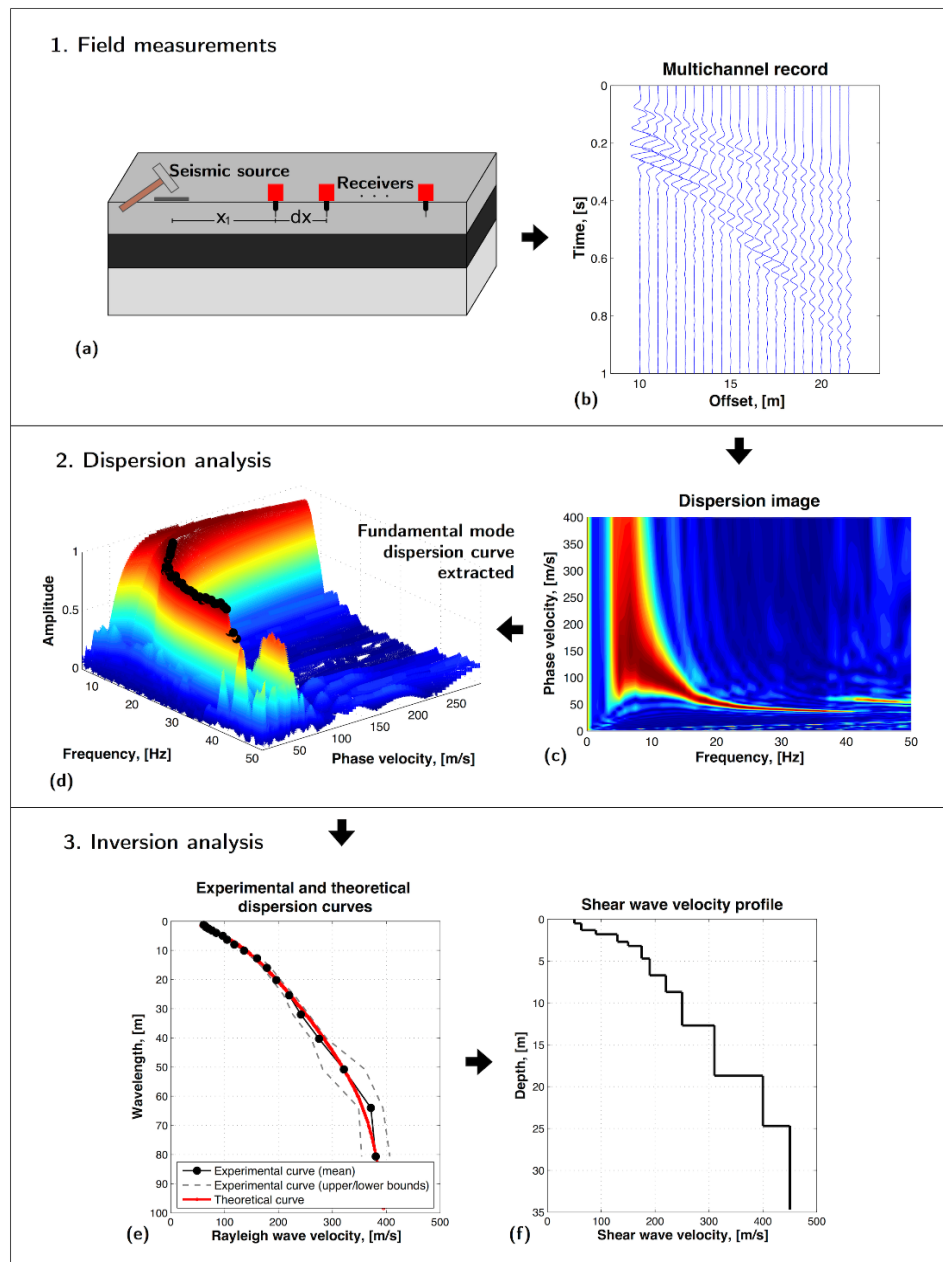


Figure 1. Overview of the MASW method. (a) Geophones are lined up on the surface of the test site. (b) A wave is generated and the wave propagation is recorded. (c) A dispersion image is obtained from the recorded surface wave data. (d) The high-amplitude bands display the dispersion characteristics and are used to construct the fundamental mode dispersion curve. (e) A theoretical dispersion curve is obtained based on assumed layer thicknesses and material parameters for each layer and compared to the experimental dispersion curve. (f) The shear wave velocity profile and the layer structure that results in an acceptable fit are taken as the results of the survey.

A Fourier transform is applied to each trace of the multichannel record. The transformed record can be expressed in terms of amplitude and phase, $\tilde{u}_j(\omega) = A_j(\omega)P_j(\omega)$. The phase term, $P_j(\omega)$, is determined by the characteristic phase velocity of each frequency component. The amplitude term, $A_j(\omega)$, preserves information regarding other properties such as

the attenuation of the signal and its geometrical spreading. As all information regarding phase velocity is contained in the phase term, the amplitude of the transformed record can be normalized in both the offset and the frequency dimensions without loss of vital information (Park et al., 1998; Ryden, Park, Ulriksen and Miller, 2004).

1. Fourier transformation and amplitude normalization

$$① \quad u_j(t) \xrightarrow{\text{FFT}} \tilde{u}_j(\omega) \quad j = 1, 2, 3, \dots, n$$

$$② \quad \tilde{u}_{j,\text{norm}}(\omega) = \frac{\tilde{u}_j(\omega)}{|\tilde{u}_j(\omega)|} = P_j(\omega)$$

2. Dispersion imaging

$$③ \quad V_{R,T} : \text{Testing Rayleigh wave phase velocity} \\ V_{R,T,\text{min}} \leq V_{R,T} \leq V_{R,T,\text{max}}$$

$$④ \quad \phi x_j : \text{Phase shifts corresponding to a given set of } \omega \text{ and } V_{R,T} \\ \phi x_j = \frac{\omega x_j}{V_{R,T}} = \frac{\omega(x_1 + (j-1)dx)}{V_{R,T}}$$

$$⑤ \quad A_s(\omega, V_{R,T}) : \text{Summed amplitude for a set of } \omega \text{ and } V_{R,T} \\ A_s(\omega, V_{R,T}) = e^{-i\phi x_1} \tilde{u}_{1,\text{norm}}(\omega) + \dots + e^{-i\phi x_n} \tilde{u}_{n,\text{norm}}(\omega)$$

⑥ Steps ④ and ⑤ repeated for varying ω and $V_{R,T}$

3. Extraction of dispersion curves

$$⑦ \quad A_s(\omega, V_{R,T}) \xrightarrow{\text{extract peak values}} \text{Dispersion curve(s)}$$

Figure 2. Overview of the phase shift method.

For a given testing phase velocity ($V_{R,T}$) and a given frequency (ω), the amount of phase shifts required to counterbalance the time delay corresponding to specific offsets are determined. The phase shifts (determined in step 4 in Fig. 2 for a given testing phase velocity) are applied to distinct traces of the transformed record that are thereafter added to obtain the slant-stacked amplitude corresponding to each pair of ω and $V_{R,T}$ (Park et al., 1998; Ryden et al., 2004). This is repeated for all the different frequency components of the transformed record in a scanning manner, changing the testing phase velocity in small increments. The dispersion image is obtained by plotting the summed amplitude in the frequency – phase velocity domain (Fig. 1c). The high-amplitude bands, which are indicated by the height of the peaks and/or a colour scale, display the dispersion characteristics of the recorded surface waves (Fig. 1d) and are used to construct the fundamental mode dispersion curve for the site (Park et al., 1998; Ryden et al., 2004). Noise is usually automatically removed in this process (Park et al., 2007).

The quality of the acquired surface wave records can be evaluated in terms of the resolution of the phase velocity spectrum, i.e. the

sharpness of the amplitude peaks observed at each frequency, the extractable frequency range and the continuity of the fundamental mode high-amplitude band.

2.3 Inversion analysis

The third step of the MASW method is to obtain a shear wave velocity profile by inversion of the fundamental mode dispersion curve. Computations are based on Rayleigh wave propagation theory assuming a plane-layered elastic earth model. The last layer is assumed to be a half-space.

Inversion problems involving the dispersion of Rayleigh waves in a layered medium must be solved by iterative methods due to their non-linearity. A theoretical dispersion curve is obtained based on an assumed number and thickness of soil layers and assumed material parameters for each layer. For a layered earth model, the shear wave velocity profile has a dominant effect on the fundamental mode dispersion curve (Xia, Miller and Park, 1999). Theoretical dispersion curves are in most cases determined by matrix methods that originate in the work of Thomson (1950) and Haskell (1953). Here, the stiffness matrix method, developed by Kausel and Roësset (1981), is used for computations of theoretical dispersion curves (Fig. 1e).

A simple local search method is employed to fit observations with theoretical predictions from assumed soil models (Ólafsdóttir, 2016). A layered soil model is suggested where the thickness of the layers increases with depth. The initial value of the shear wave velocity for each layer is estimated from the measured dispersion curve. It is based on the ratio between the propagation velocities of Rayleigh waves and shear waves in a homogeneous medium, and a simple relation between Rayleigh wave wavelength and representative depth (Kramer, 1996; Park et al., 1999). Other model parameters, i.e. Poisson's ratio (or the compressional wave velocity) and the mass density of each layer, are either estimated based on independent soil investigations or on experience of similar soil types from other sites. The shear wave velocity of each layer is updated during the inversion process while all other model parameters are kept unchanged. In each iteration, the misfit between the theoretical dispersion

curve and the experimental dispersion curve is evaluated in terms of the root-mean-square (RMS) error between the theoretical and experimental Rayleigh wave phase velocities. The shear wave velocities obtained by this approach, along with the layer thicknesses, are then used to represent the soil profile at the survey site (Fig. 1f).

2.4 Measurement profile configuration

It is commonly recognised that the configuration of the MASW measurement profile can affect the quality of the surface wave records that are obtained (Park and Carnevale, 2010; Park, Miller and Miura, 2002; Park, Miller and Xia, 2001). The main parameters related to the setup of the measurement profile are the length of the receiver spread (or the receiver spacing if a fixed number of geophones is used) and the source offset.

The length of the receiver spread is related to the longest Rayleigh wave wavelength that is obtained during data acquisition and therefore also related to the maximum depth of investigation:

$$\lambda_{max} \approx L \quad (2)$$

where λ_{max} (m) is the longest wavelength and L (m) is the length of the receiver spread.

Attempts to analyse longer wavelengths than indicated by Eq. (2) can lead to less accurate results. A recent study has shown that the fluctuating inaccuracy will although be within 5% for $L \leq \lambda_{max} \leq 2L$ (Park and Carnevale, 2010).

The minimum source offset required to avoid undesirable near-field effects, i.e. the risk of non-planar surface waves being picked up by the receivers, depends on the longest wavelength that is analysed. It is commonly regarded that plane-wave propagation of surface waves first occurs when the source offset is greater than half the longest wavelength. However, studies have shown that this criterion can be relaxed significantly for MASW surveys (Park et al., 1999; 2002).

3 MASW FIELD MEASUREMENTS

MASW field measurements were carried out in August 2014 at two test sites at Bakkafjara in South Iceland, referred to as sites B1 and B2 (see Fig. 3). The soil at Bakkafjara is mainly uniformly graded dark basalt sand. The groundwater table is estimated to be at a 4.0 m depth (Ólafsdóttir, 2016).

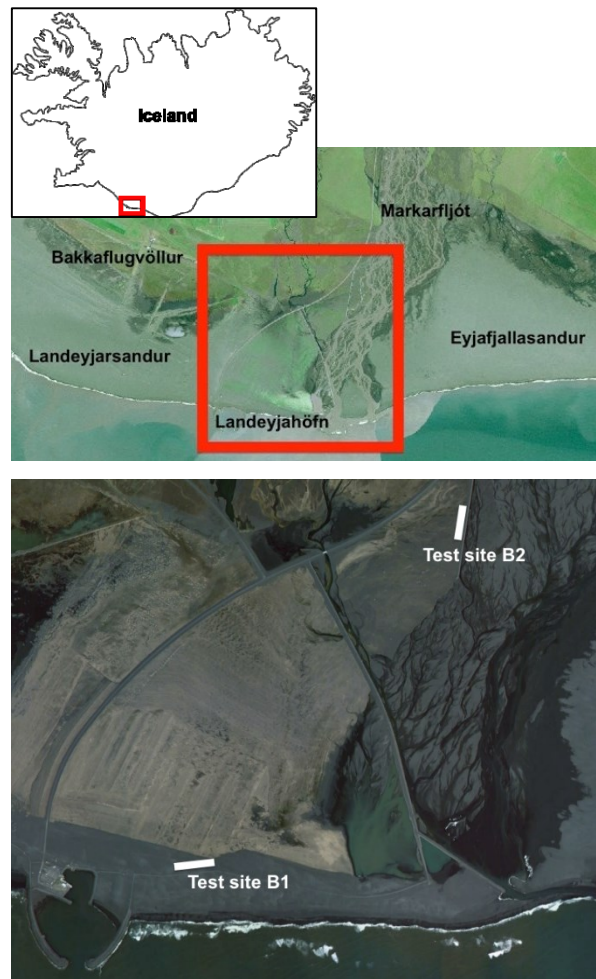


Figure 3. Location of MASW field measurements at Bakkafjara in South Iceland. Data were acquired at two test sites, referred to as test site B1 and test site B2.

The field measurements at Bakkafjara were performed using twenty-four 4.5 Hz geophones as receivers. A 6.3 kg sledgehammer and a single jump at the end of the measurement profile were used as impact sources. At each test site, three receiver spreads with the same midpoint but different receiver spacing, i.e. $dx \in \{0.5, 1.0, 2.0\}$ m, were tested.

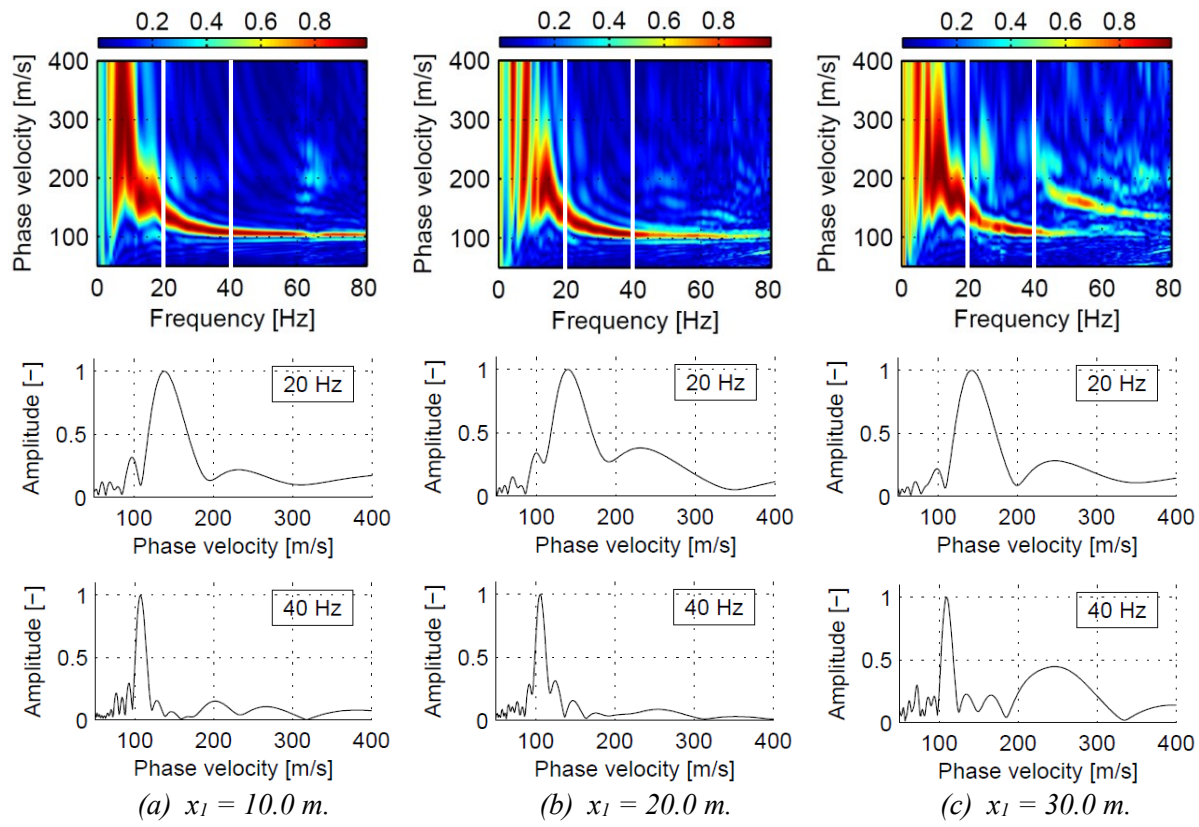


Figure 4. Change in spectral resolution with length of source offset. Top: Typical dispersion images obtained at Bakkafjara test site B2 with a receiver spread of length $L = 23.0 \text{ m}$ ($dx = 1.0 \text{ m}$) and a source offset of (a) $x_I = 10.0 \text{ m}$, (b) $x_I = 20.0 \text{ m}$ and (c) $x_I = 30.0 \text{ m}$. A 6.3 kg sledgehammer was used as an impact source. Middle/bottom: Cross sections through the dispersion images at $f = 20 \text{ Hz}$ and $f = 40 \text{ Hz}$. The location of the cross sections is indicated by vertical lines in Fig. 4 (top).

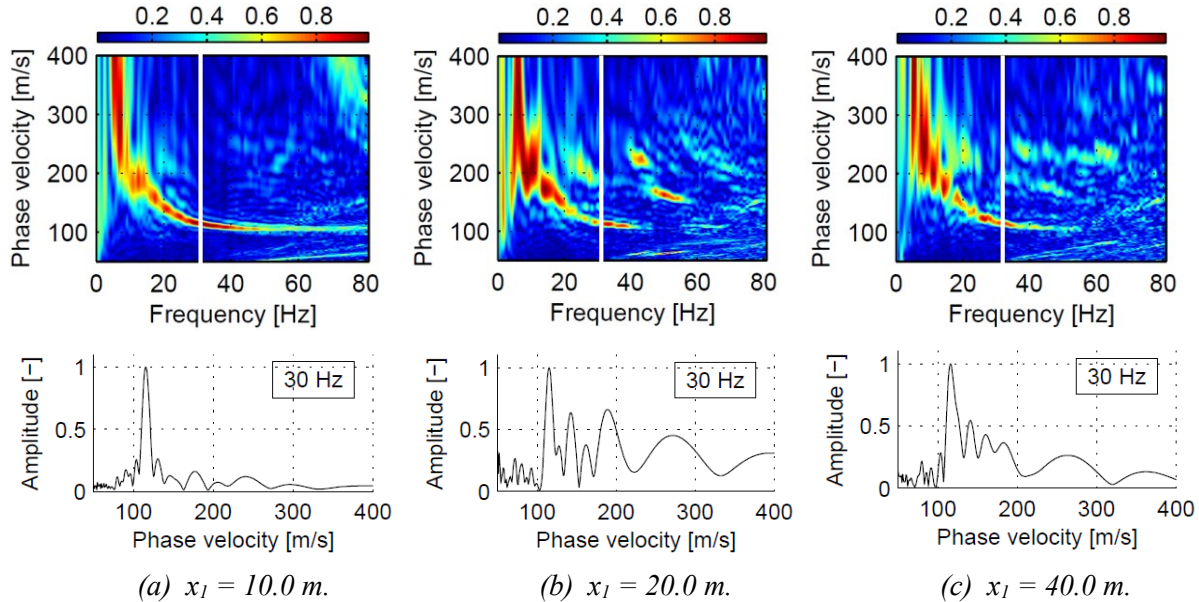


Figure 5. Change in spectral resolution with length of source offset. Top: Typical dispersion images obtained at Bakkafjara test site B2 with a receiver spread of length $L = 46.0 \text{ m}$ ($dx = 2.0 \text{ m}$) and a source offset of (a) $x_I = 10.0 \text{ m}$, (b) $x_I = 20.0 \text{ m}$ and (c) $x_I = 40.0 \text{ m}$. A 6.3 kg sledgehammer was used as an impact source. Bottom: Cross sections through the dispersion images at $f = 30 \text{ Hz}$.

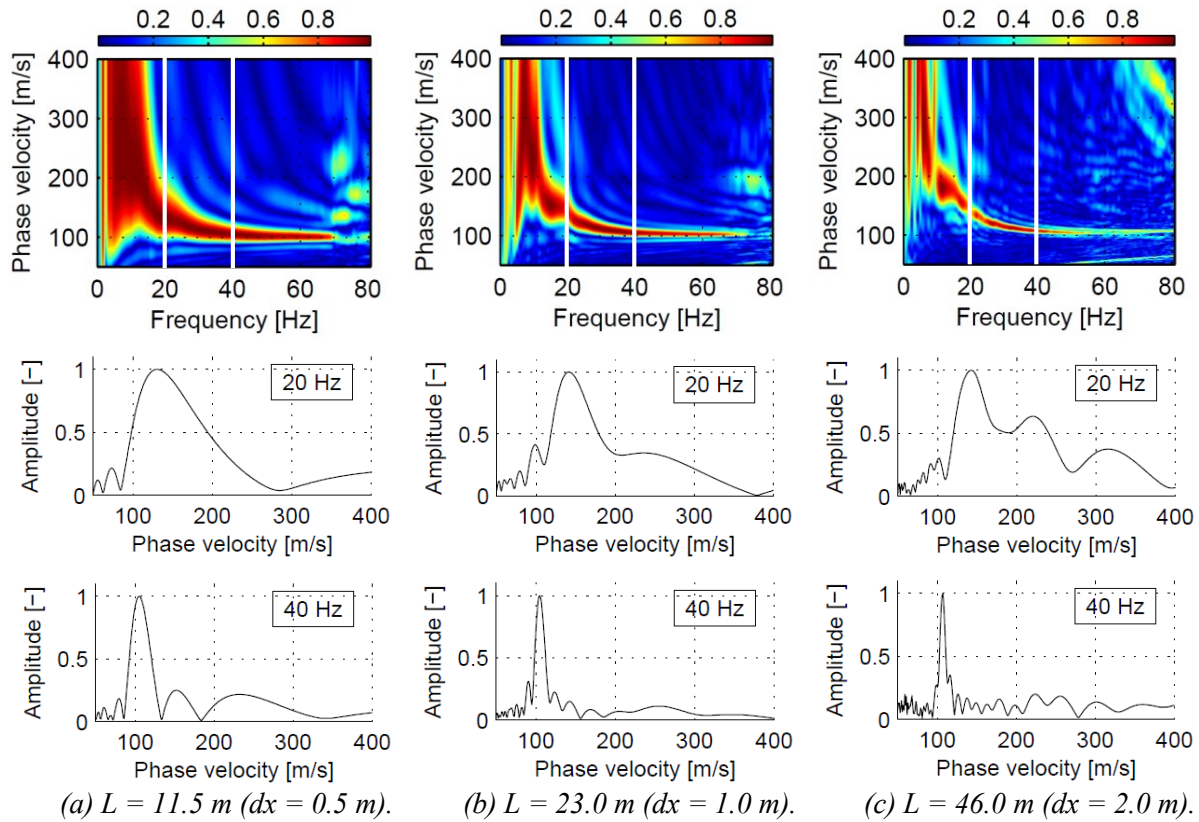


Figure 6. Change in spectral resolution with length of receiver spread. Top: Typical dispersion images obtained at Bakkafjara test site B2 with receiver spreads of length (a) $L = 11.5 \text{ m}$, (b) $L = 23.0 \text{ m}$ and (c) $L = 46.0 \text{ m}$. The source offset is $x_1 = 5.0 \text{ m}$ in all cases. A 6.3 kg sledgehammer was used as an impact load. Middle/bottom: Cross sections through the dispersion images at $f = 20 \text{ Hz}$ and $f = 40 \text{ Hz}$.

For each receiver setup, up to seven source offsets in the range of 5 m to 50 m were used. No systematic difference was observed between surface wave records where the impact load was created by a sledgehammer and where it was created by a jump.

3.1 Observed effects of measurement profile configuration at Bakkafjara

Typical dispersion images of records acquired at the Bakkafjara test site B2 with receiver spreads of fixed length (23.0 m in Fig. 4 and 46.0 m in Fig. 5) but with source offsets of various lengths are shown in Figs. 4 (top) and 5 (top). A 6.3 kg sledgehammer was used as an impact source in all cases. Figures 4 and 5 (middle and bottom) show the variation of the amplitude band with Rayleigh wave phase velocity at frequencies 20 and 40 Hz (Fig. 4) and 30 Hz (Fig. 5). The amplitude band is normalized such that the maximum amplitude at each

frequency is one. The highest peaks correspond in all cases to the identified fundamental mode.

The results presented in Figs. 4 and 5 indicate that the length of the source offset did not have a strong effect on the sharpness of the amplitude peaks. The same was observed based on data acquired at the Bakkafjara test site B1. However, for a given length of the receiver spread, an increased length of the source offset tended to cause increased disturbances in the spectral high-amplitude band. Moreover, the presence of overtones and/or other noise became more evident in the higher frequency range of the phase velocity spectrum with increasing source offset.

Figure 6 (top) shows typical dispersion images obtained at test site B2 with receiver spreads of length (a) 11.5 m, (b) 23.0 m and (c) 46.0 m. The source offset was 5.0 m in all cases. The impact load was created by a sledgehammer. Cross sections through the dispersion images at frequencies 20 and 40 Hz

are shown in Fig. 6 (middle and bottom). The highest peaks correspond to the fundamental mode.

Based on the results presented in Fig. 6, the length of the receiver spread had a substantial effect on the resolution of the dispersion image. In general, by lengthening the receiver spread (i.e. increasing the receiver spacing and keeping the number of geophones used for recording unchanged), the fundamental mode high-amplitude peaks appeared sharper and better separation of overtones was observed. The same was noticed by analysis of surface wave records acquired at test site B1. At the Bakkafjara test sites, records acquired with a 46.0 m long receiver spread allowed in general extraction of the fundamental mode dispersion curve at lower frequencies than records acquired with receiver spreads of length 11.5 m or 23.0 m. However, the dispersion images presented in Fig. 6 (top) indicate that increased length of the receiver spread tended to have a negative effect on the continuity of the fundamental mode high-amplitude band, especially in the higher frequency range, which counteracted to some extent the benefits of increasing the length of the receiver spread.

4 DISCUSSION

Based on the results acquired at the Bakkafjara test sites, dispersion images of records acquired with a short receiver spread and/or a short/medium-length source offset showed in most cases a relatively unbroken fundamental mode high-amplitude band and allowed identification and extraction of the fundamental mode dispersion curve in the higher frequency range. Hence, time series recorded by a relatively short measurement profile provided in general the most information about the dispersion properties of the short wavelength wave components that propagated through the top-most soil layers.

The high-amplitude band observed in a dispersion image acquired with a short receiver spread can be very wide, especially at the low- and mid-range frequencies. The low spectral resolution can cause difficulties in identification of the spectral peak values, which risks less accurate dispersion curves. In general, by lengthening the receiver spread, the observed

spectral resolution increases, which facilitates the identification and the extraction of the fundamental mode dispersion curve, especially in the lower frequency range. Hence, the study found that time series recorded by long receiver spreads tended to provide the most investigation depth.

The observed effects of the data acquisition parameters suggest that an increased range in investigation depth can be obtained by combining dispersion curves acquired with measurement profiles of different lengths. Furthermore, combining several dispersion curves creates possibilities to estimate the accuracy of the extraction process, to compensate for segments of missing data in the extracted dispersion curves and to diminish the effect of poor quality surface wave records without the analyst having to selectively choose records for further analysis.

The dispersion analysis software tool that is under development includes a special algorithm to obtain an average experimental dispersion curve, along with upper and lower boundary curves (Ólafsdóttir, 2016). The average dispersion curve is obtained by grouping data points from multiple dispersion curves together within 1/3 octave wavelength intervals. All phase velocity values within each interval are added up and their mean used as an estimate of the phase velocity of Rayleigh wave components belonging to the given wavelength range. Upper and lower boundaries for the average dispersion curve are obtained using the standard deviation of the values within each wavelength band. The average dispersion curve, along with its upper and lower boundaries, is subsequently used as an input in the inversion analysis.

The average experimental dispersion curves obtained for the Bakkafjara test sites B1 and B2 by using the aforementioned methodology are shown in Figs. 7a and 8a. The upper and lower bounds correspond to plus/minus one standard deviation of the average curve. Inversion was then used to obtain the shear wave velocity profiles for the sites (see Figs. 7b and 8b).

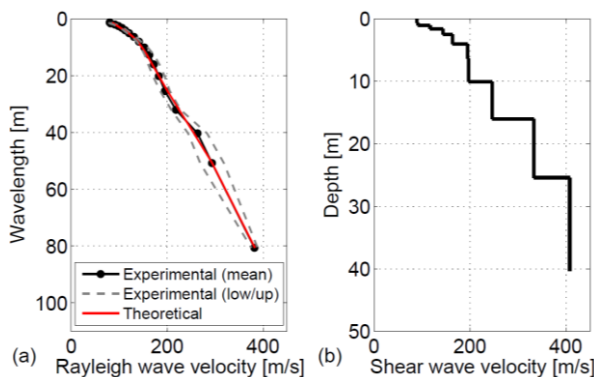


Figure 7. (a) Comparison of experimental and theoretical dispersion curve based on inversion. (b) The estimated shear wave velocity profile for the Bakkafjara test site B1.

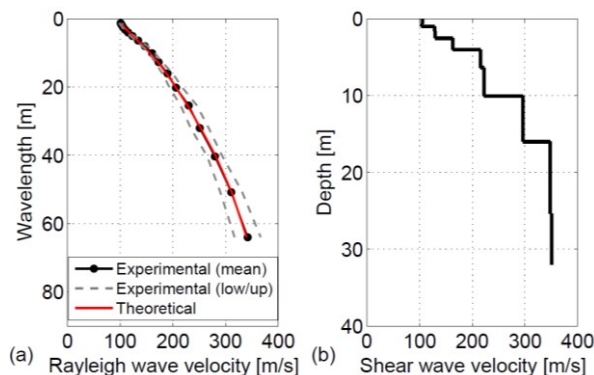


Figure 8. (a) Comparison of experimental and theoretical dispersion curve based on inversion. (b) The estimated shear wave velocity profile for the Bakkafjara test site B2.

5 CONCLUSIONS AND SUMMARY

MASW is a relatively new seismic exploration method to estimate the shear wave velocity profile of near-surface materials. MASW measurements have been carried out at two test sites at Bakkafjara in South Iceland using twenty-four 4.5 Hz geophones for recording. For each receiver setup, up to seven different source offsets were used, ranging from 5 m to 50 m. Dispersion analysis was then applied to evaluate a phase velocity spectrum and a dispersion curve based on each surface wave record that was acquired.

The results indicated that the configuration of the MASW measurement profile had a substantial effect on the acquired surface wave data. Records obtained using a relatively short measurement profile provided in general the

most information about the dispersion properties of the short wavelength wave components that propagated through the top-most soil layers. However, time series recorded by long receiver spreads provided in general the most investigation depth. The observations are in accordance to existing recommendations where the obtainable investigation depth is suggested to be directly related to the length of the receiver spread.

Analysis of the dispersion images and the dispersion curves indicated that it is beneficial to combine results from several measurements which have been carried out using measurement profiles of different lengths prior to the inversion analysis. A new algorithm has been developed to compute an average experimental dispersion curve, along with upper and lower boundaries, by adding up dispersion curves obtained based on multiple surface wave registrations. The new data processing procedure has been applied to the data acquired at the Bakkafjara test sites to evaluate average dispersion curves for wavelengths up to 80 m.

Optimum values of measurement profile setup parameters for MASW surveys are to some extent documented in references. An effort is though necessary to collect more information about the optimal setup, since there are many site-specific factors that may affect the setup, for instance the depth to bedrock and the soil type. Future research topics include further and more detailed analysis of the effects of the measurement profile configuration and development of guidelines for the setup of the measurement profile(s) and the execution of the MASW measurements in the field.

6 ACKNOWLEDGEMENTS

The project is financially supported by grants from the University of Iceland Research Fund, the Icelandic Road and Costal Administration and the Energy Research Fund of the National Power Company of Iceland.

7 REFERENCES

Bessason, B., Baldvinsson, G. I., & Þórarinsson, Ó. (1998). SASW for evaluation of site-specific earthquake excitation. Proceedings of the 11th European Conference on Earthquake Engineering, CD-ROM, Paris, Paris.

Bessason, B., & Erlingsson, S. (2011). Shear wave velocity in surface sediments. *Jökull*, 61, 51-64.

CEN. (2004). EN1998-1:2004, Eurocode 8: Design of structures for earthquake resistance - Part 1: General rules, seismic actions and rules for buildings. Brussels: European Committee for Standardization.

Haskell, N. A. (1953). The dispersion of surface waves on multilayered media. *Bulletin of Seismological Society of America*, 43(1), 17-34.

Kausel, E., & Roësset, J. M. (1981). Stiffness matrices for layered soils. *Bulletin of the Seismological Society of America*, 71(6), 1743-1761.

Kramer, S. L. (1996). Geotechnical Earthquake Engineering. Upper Saddle River, NJ: Prentice Hall.

Ólafsdóttir, E. Á, Bessason, B. & Erlingsson S (2015). MASW for assessing liquefaction of loose sites. Proceedings of the 16th European Conference on Soil Mechanics and Geotechnical Engineering, 13-17 September 2015, Edinburgh, UK.

Ólafsdóttir, E. Á. (2016). Multichannel Analysis of Surface Waves for assessing soil stiffness. (Unpublished master's thesis). Faculty of Civil and Environmental Engineering, University of Iceland, Reykjavík, Iceland.

Park, C. B., Miller, R. D., & Xia, J. (1998). Imaging dispersion curves of surface waves on multichannel record. 68th Annual International Meeting Society of Exploration Geophysicists, Expanded Abstracts, 1377-1380.

Park, C. B., Miller, R. D., & Xia, J. (1999). Multichannel analysis of surface waves. *Geophysics*, 64(3), 800-808.

Park, C. B., Miller, R. D., & Xia, J. (2001). Offset and resolution of dispersion curve in multichannel analysis of surface waves (MASW). Proceedings of the Symposium on the Application of Geophysics to Engineering and Environmental Problems (SAGEEP 2001), Denver, Colorado, SSM-4.

Park, C. B., Miller, R. D., & Miura, H. (2002). Optimum field parameters of an MASW survey. Expanded Abstracts, SEG-J, Tokyo, May 22-23, 2002.

Park, C. B., Miller, R. D., Xia, J., & Ivanov, J. (2007). Multichannel analysis of surface waves (MASW) - active and passive methods. *The Leading Edge*, 26(1), 60-64.

Park, C. B., & Carnevale, M. (2010). Optimum MASW Survey - Revisit after a Decade of Use. In Fratta, D. O., Puppala, A. J., & Muhunthan, B. (editors), *GeoFlorida 2010: Advances in Analysis, Modeling and Design*, 1303-1312, doi: 10.1061/41095(365)130.

Ryden, N., Park, C. B., Ulriksen, P., & Miller, R. D. (2004). Multimodal approach to seismic pavement testing. *Journal of Geotechnical and Geoenvironmental Engineering*, 130, 636-645.

Thomson, W. T. (1950). Transmission of elastic waves through a stratified solid medium. *Journal of Applied Physics*, 21(2), 89-93.

Xia, J., Miller, R. D., & Park, C. B. (1999). Estimation of near-surface shear-wave velocity by inversion of Rayleigh waves. *Geophysics*, 64(3), 691-700.

Xia, J., Miller, R. D., Park, C. B., & Ivanov, J. (2000). Construction of 2-D vertical shear-wave velocity field by the multichannel analysis of surface waves technique. Proceeding of the Symposium of the Application of Geophysics to Engineering Environmental Problems (SAGEEP 2000) Arlington, VA., February 20-24, 1197-1206.

Xia, J., Miller, R. D., Park, C. B., Hunter, J. A., Harris, J. B., & Ivanov, J. (2002). Comparing shear-wave velocity profiles from multichannel analysis of surface wave with borehole measurements. *Soil Dynamics and Earthquake Engineering*, 22(3), 181- 190.